Oral Oncology 90 (2019) 94–101

Contents lists available at ScienceDirect

Oral Oncology

journal homepage: www.elsevier.com/locate/oraloncology

A functional gene expression analysis in epithelial sinonasal cancer: Biology and clinical relevance behind three histological subtypes

Loris De Cecco[a], Mara Serena Serafini[a], Carla Facco[b], Roberta Granata[c], Ester Orlandi[d], Carlo Fallai[d], Lisa Licitra[c,e], Edoardo Marchesi[a], Federica Perrone[f], Silvana Pilotti[f], Pasquale Quattrone[f], Cesare Piazza[g], Fausto Sessa[b], Mario Turri-Zanoni[h], Paolo Battaglia[h], Paolo Castelnuovo[h], Paolo Antognoni[i], Silvana Canevari[a], Paolo Bossi[c,*]

[a] Integrated Biology Platform, Department of Applied Research and Technology Development, Fondazione IRCCS Istituto Nazionale dei Tumori di Milano, Italy
[b] Department of Pathology, University of Insubria and ASST Sette Laghi, Ospedale di Circolo, Varese, Italy
[c] Head and Neck Medical Oncology Department, Fondazione IRCCS Istituto Nazionale dei Tumori di Milano, Milan, Italy
[d] Radiation Oncology Department, Fondazione IRCCS Istituto Nazionale dei Tumori di Milano, Milan, Italy
[e] University of Milan, Italy
[f] Department of Pathology and Laboratory Medicine, Fondazione IRCCS Istituto Nazionale dei Tumori di Milano, Milan, Italy
[g] Department of Otorhinolaryngology, Maxillofacial and Thyroid Surgery, Fondazione IRCCS Istituto Nazionale dei Tumori di Milano, University of Milano, Milan, Italy
[h] Department of Otorhinolaryngology, University of Insubria and ASST Sette Laghi, Ospedale di Circolo, Varese, Italy
[i] Department of Radiotherapy, ASST Sette Laghi, Ospedale di Circolo, Varese, Italy

ARTICLE INFO

Keywords:
Sinonasal epithelial cancer
Gene expression
Cancer biology
Tumor microenvironment
Neuroendocrine signature

ABSTRACT

Epithelial sinonasal cancers (SNCs) are rare diseases with overlapping morphological features and a dismal prognosis. We aimed to investigate the expression differences among the histological subtypes for discerning their molecular characteristics.

We selected 47 SNCs: (i) 21 nonkeratinizing squamous cell carcinomas (NKSCCs), (ii) 13 sinonasal neuroendocrine cancers (SNECs), and (iii) 13 sinonasal undifferentiated cancers (SNUCs). Gene expression profiling was performed by DASL (cDNA-mediated annealing, selection, extension, and ligation) microarray analysis with internal validation by quantitative RT-PCR (RT-qPCR). Relevant molecular patterns were uncovered by sparse partial-least squares discriminant analysis (sPLS-DA), microenvironment cell type (xCell), CIBERSORT, and gene set enrichment (GSEA) analyses.

The first two sPLS-DA components stratified samples by histological subtypes. xCell highlighted increased expression of immune components ($CD8^+$ effector memory cells, in SNUC) and "other cells": keratinocytes and neurons in NKSCC and SNEC, respectively. Pathway enrichment was observed in NKSCC (six gene sets, proliferation related), SNEC (one gene set, pancreatic β-cells), and SNUC (twenty gene sets, some of them immune-system related). Major neuroendocrine involvement was observed in all the SNEC samples.

Our high-throughput analysis revealed a good diagnostic ability to differentiate NKSCC, SNEC, and SNUC, but indicated that the neuroendocrine pathway, typical and pathognomonic of SNEC is also present at lower expression levels in the other two histological subtypes. The different and specific profiles may be exploited for elucidating their biology and could help to identify prognostic and therapeutic opportunities.

Introduction

The sinonasal tract can develop a wide variety of tumors, with a greater heterogeneity of neoplasms than that in any other part of the human body [1]. Sinonasal tumors are rare diseases, representing approximately 5% of all head and neck neoplasms [2]. According to RARECARE, their worldwide annual incidence is ~0.5 cases per 100,000 people [3], and the average age at which patients present with such lesions is between 50 and 60 years [4]. These cancers require a multimodal therapeutic approach, including surgical treatment, radiation, and systemic chemotherapy. Despite the aggressive treatment, globally the prognosis of patients remains poor, with an overall 5-year survival rate of 30–50% [5]. The most frequent histological kind of sinonasal tumors is the epithelial type [4], which differs from epithelial

* Corresponding author at: Fondazione IRCCS Istituto Nazionale dei Tumori di Milano, Via Venezian 1, 20133 Milan, Italy.
E-mail address: paolo.bossi@istitutotumori.mi.it (P. Bossi).

https://doi.org/10.1016/j.oraloncology.2019.02.003
Received 10 September 2018; Received in revised form 22 January 2019; Accepted 2 February 2019
Available online 11 February 2019

cancers arising from the mucosa of other head-and-neck subsites in epidemiological, clinical, and causal factors [5]. Due to their rapid growth, most of epithelial sinonasal cancers (SNCs) are detected and treated at advanced stages. In terms of a histological definition, they are characterized by a high rate of discrepancies after second-opinion review [6]. As a matter of fact, pathologists may have difficulty differentiating the SNC subtypes owing to the overlaps of morphological features and the similarity of immunohistochemical (IHC) characteristics, all increasing the laboriousness of the diagnosis. Even though several IHC markers have been proposed to overcome the complexity of the classification, no consensus on this subject has been reached yet. Clearly, to better define the prognosis and treatment options for SNCs, it is crucial to dissect their heterogeneity and obtain valuable information on the biology of these malignant tumors. According to recent data, the mutational profiles could help to identify patterns of alterations typical of each histological type and to regroup different tumors [2]. Because SNCs are a rare entity, the identified genomic alterations are limited to the NUT-BRD4 translocation in NUT carcinoma (target of bromodomain and extra-terminal inhibitors) [7] and an EGFR exon 20 mutation (target of second and third generations of EGFR inhibitors) in squamous cell carcinoma [8]. Another remarkable observation is that no comprehensive analyses of the gene expression of the three histological subtypes are available at present. The present work was focused on gene expression analysis of different and challenging epithelial subtypes [1]. We analyzed a retrospective series of SNCs representative of the three selected histological subtypes, which manifested overlapping morphological features: (i) nonkeratinizing squamous cell carcinoma (NKSCC), a subtype of squamous cell carcinoma; (ii) sinonasal neuroendocrine carcinoma (SNEC), characterized by neuroendocrine features; and (iii) sinonasal undifferentiated carcinoma (SNUC), with an undetermined histogenesis without evidence of squamous or glandular differentiation, and therefore representing a category with a diagnosis of exclusion [2,9]. The aim of our work was to find out whether gene expression may be of some help in refining the three histological subtypes by uncovering possible different and specific profiles that may be exploited for elucidating their biology and for improving treatment approaches.

Patients and methods

Patients and samples

We selected 47 cases from a retrospective cohort of SNCs cases (treated at two Italian referral centers: Fondazione IRCCS Istituto Nazionale dei Tumori, Milan and Ospedale di Circolo, Varese) according to the following criteria: (i) histological patterns consistent with NKSCC, SNUC, or SNEC, according to WHO [10]; (ii) not having received any other treatment for the index disease, except for diagnostic biopsies; (iii) not having received any previous radiation therapy in the head-and-neck area; and (iv) availability of sufficient histological material.

The local Ethical Committee approved the study design, and according to our practice, all patients signed an informed consent form for the use of their data for research purposes. Patients' medical records were retrospectively reviewed to identify the following clinical characteristics: age and gender, disease stage and subsite, and the therapeutic approach applied. We analyzed a series of patients treated between 01/2000 and 04/2016. Patients were staged or reclassified according to the VII edition of the American Joint Committee on Cancer Staging [11]. All pathological specimens were reviewed by an internal pathologist expert in head and neck cancer (S.P.).

RNA isolation and gene expression profiling

The gene expression profiling was performed starting from formalin-fixed paraffin-embedded (FFPE) material from diagnostic biopsies obtained by direct manual dissection of methylene blue–-stained slices and containing at least 75% of tumor cell content without necrosis or surrounding normal tissue. Total RNA was isolated using the miRNeasy FFPE Kit (Qiagen, Valencia, CA, USA), and the procedure was automated on a QIAcube Robotic workstation. Extracted material was quantified on a Nanodrop-1000 instrument (Thermo Fisher Scientific, Waltham, MA, USA). RNA quality was assessed by RT-qPCR analysis of amplicons of different sizes for the *ACTB* housekeeping gene [12,13]. Total RNA (200 ng) from each sample was profiled (as described by Bossi et al. [14]) for gene expression by the Human WG-DASL (cDNA-mediated annealing, selection, extension, and ligation) assay technology with Human HT12 v4.0 BeadChips (Illumina Inc., San Diego, CA, USA) allowing for the detection of 29,377 transcripts. Reverse transcription, oligo annealing, ligation, amplification, labeling, probe purification, hybridization, and chip washing were performed following the manufacturer's instructions. Microarray chips were scanned with an Illumina BeadArray Reader. All microarray data are MIAME compliant, and the raw data were deposited in the NCBI Gene Expression Omnibus (GEO) database [15] under the accession number GSE118386. Bioinformatics analyses were performed in R software (R Development Core Team, 2007 version 3.5.1), BioConductor [16], and BRB-ArrayTool developed by Richard Simon and by the BRB-ArrayTools Development Team (v4.6.0; National Cancer Institute, USA); details are presented in Supplementary File 1.

Results

Case material

Clinical and pathological characteristics of the present series of patients are described in Table 1. We analyzed the database of patients with NKSCC, SNEC, or SNUC treated between 1/2000 and 4/2016. We identified 65 cases; sufficient histological samples were available for 47 patients on whose biopsies the following diagnoses were made: NKSCC, 21 cases (44%); SNEC, 13 (27%), and SNUC, 13 cases (27%). Male prevalence (74%) and 58 years as a median age (range, 16–84) are in line with the epidemiological data reported in the literature [17–19]. No female was found affected by SNEC, possibly owing to the small sample size. The main subsite of origin was the ethmoid (62%), followed by the nasal cavity (26%) and maxillary and other subsites (6% each). Locally advanced (III–IV) stages were the most prevalent (91%), mainly due to the advanced T values (T4a, 19%; T4b, 53%). Treatment consisted of surgical resection (followed by radiation with or without concurrent chemotherapy) or of curative chemoradiation, preceded by induction chemotherapy in case of very advanced tumors. No difference in treatment was observed among the histotypes.

Gene expression patterns in SNCs

Fig. 1 depicts the analyses applied in the present study based on gene expression profiling aimed at improving our knowledge about the biology behind the three selected SNC histological subtypes. A microarray platform was used for gene expression analysis yielding a data matrix containing 17,531 unique genes. Among the available bioinformatics tools, we decided to apply sparse partial-least squares discriminant analysis (sPLS-DA): a supervised, pattern-recognition approach enabling to reduce the dimensionality of data [20] and already successfully used in head and neck squamous cell carcinoma (HNSCC) genomic translational research [21]. Because our study deals with a multiclass histological stratification with a small sample size as compared to the large number of genes, sPLS-DA allows for retaining those genes showing the best performance on discriminating NKSCC, SNEC, and SNUC histological features. For this purpose, we determined the optimal number of dimensions and genes on the basis of the lowest misclassification rate. The best performance was achieved by including the first two components: (i) the first component, n = 72 genes; (ii) the

Table 1
Main clinical–pathological characteristics of the analyzed patients.

Clinical-pathological characteristics		All SNCs N = 47	NKSCC N = 21	SNEC N = 13	SNUC N = 13	P value
Age, years	Median (range)	58 (16–84)	64 (39–77)	52 (16–84)	50 (31–78)	0.241[a]
Gender	Male	35	13	13	9	0.041[b]
	Female	12	8	/	4	
Site	Nasal cavity	12	4	3	5	0.696[b]
	Ethmoid sinus	29	13	9	7	
	Maxillary sinus	3	2	1	/	
	Other	3	2	/	1	
T stage	1	1	/	/	1	0.255[b]
	2	4	2	1	1	
	3	8	4	3	1	
	4a	9	7	/	2	
	4b	25	8	9	8	
Stage	I–II	4	1	1	2	0.818[b]
	III	8	4	2	2	
	IV	35	16	10	9	
Therapy	Surgery ± RT ± CT	33	17	9	7	0.243[b]
	CTRT ± induction CT	14	4	4	6	

SNC: sinonasal cancer; NKSCC: non-keratinizing squamous cell carcinoma; SNEC: sinonasal neuroendocrine carcinoma; SNUC: sinonasal undifferentiated carcinoma; CT: chemotherapy; RT: radiation.
T stage at first diagnosis according to the TNM 7th edition.
[a] P-value as Kruskal–Wallis test.
[b] P-value as $\chi 2$ tests.

second component, n = 10 genes. The two gene lists are given in Table A1, and the first and second component loading values are depicted in Figs. A1 and A2, respectively (a list of functionally relevant genes is highlighted in Table 2). According to this approach, a total of 82 genes subdivided into two components were able to stratify SNC tumor samples into the three histological subtypes (Fig. 2a). The first component significantly separated SNEC from NKSCC and SNUC (Fig. 2b), while the second component stratified histological subtypes NKSCC and SNUC (Fig. 2c). The classification performance of the two components, on the basis of the selected parameters, was evaluated by estimating the receiver-operating characteristic (ROC) curves and by assessing the area under the curve (AUC). In the three different comparisons considering one histological subtype versus the others, the discriminative ability of sPLS-DA reached at least AUC > 0.95 (Fig. 2d).

The tumor microenvironment landscape

We used the xCell tool to portray the infiltrate of "immune cells," "stromal cells," and "other cells" (components) present in each sample. The different sets of cell types were plotted according to their scores, with a dimensionality reduction technique and colored by subtype, as shown in Fig. 3a the subtypes are clearly separated. Among the 64 cell types, we found significantly different contents among the three histotypes: the immune component ($CD8^+$ effector memory T cells, P value = 0.0014; mast cells, P value = 0.00241) showed a significant increase in proportion within SNUC (Figure 3b) and moderate enrichment in NKSCC; NKSCC manifested an increase in the proportion of "other cells," namely epithelial cells (keratinocytes and sebocytes, P value = 0.00249 and P value = 0.0135 respectively); SNEC showed enrichment in "other cells" (neurons, P value = 0.00612; Fig. 3c).

Visualization of infiltrates of the immune and "other cells" in SNCs as assessed by xCell; individual patients are summarized based on two-dimensional coordinates from t-distributed stochastic neighbor embedding (t-SNE) and are colored by subtype.

Quantitative RT-PCR (RT-qPCR) validation

We carried out RT-qPCR for internal validation of the selected

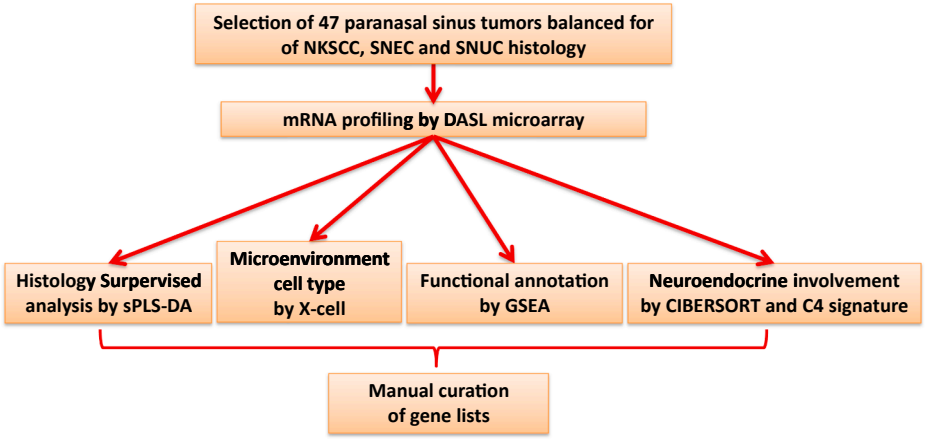

Fig. 1. Study workflow.

Table 2
Summary of the main characteristics of the SNEC subtypes identified by genomic analyses.

Genomic analysis		Sinonasal epithelial cancer subtytes		
		NKSCC	SNEC	SNUC
sPLS-DA Identification of specific gene(s) in component:		First: DSG2, TMEM123	First: NRSN1, TLGLN3, SYT4, SYT13, CHGA, SYP MIR758	
		Second: LINC00461		Second: RGS1
Functional pathways	Vs the other two	MYC targets; Mitotic spindle	Pancreas beta cells	Innate and adaptive immune response; Epithelial mesenchymal transition; KRAS up; Hypoxia; TP53; Cholesterol homeostasis
Neuroendocrine involvement		> 50% = 1/21 > 25% = 4/21	> 50% = 13/13 > 25% = 13/13	> 50% = 1/13 > 25% = 3/13
	Pan-cancer C4	Heterogeneous distribution		
Agreement with previously reported IHC markers		Not applicable	YES	Not applicable

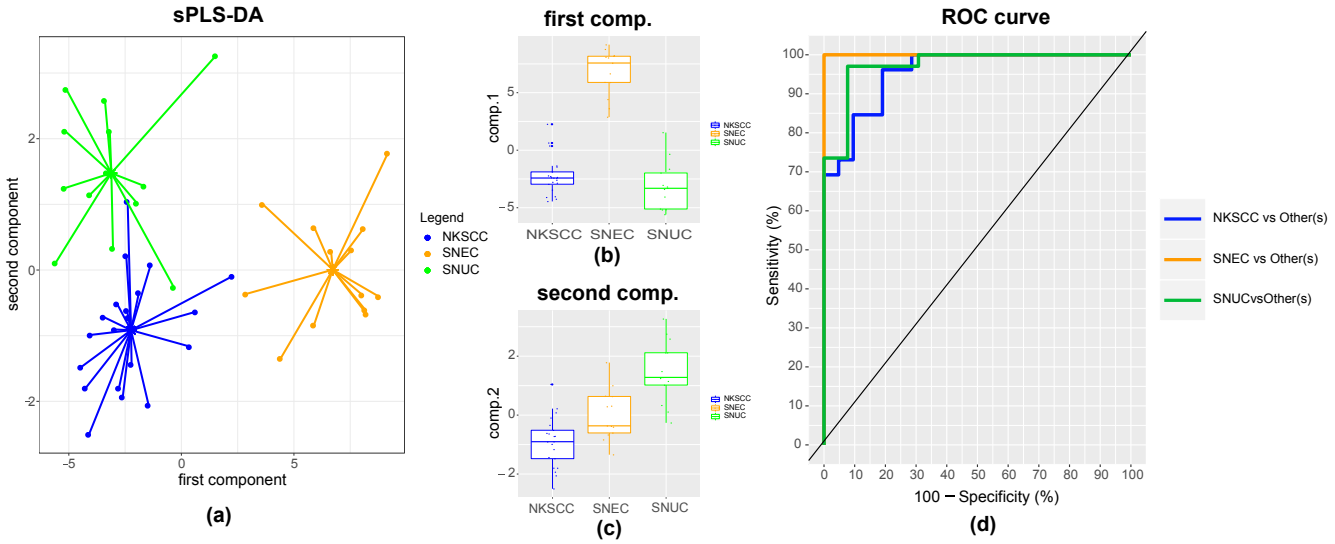

Fig. 2. Gene expression patterns in SNCs. (a) sPLS-DA allows for selection of genes that best separate SNUC (n = 13), SNEC (n = 13), and NKSCC (n = 21); the sPLS-DA score plot of the first two components including 72 and 10 genes, respectively, is shown, and data on each individual patient are plotted. The lines indicate the distance from the respective centroid to the samples of each class. (b) Box plots of the loading values for the first component divided on the basis of the three histological subtypes; significant differences were observed in the comparisons SNEC/NKSCC (P value = 3.52E−15) and SNEC/SNUC (P value = 9.88E−12). (c) Box plots of the loading values for the second component; significant differences were observed in comparisons SNEC/NKSCC (P value = 0.00465), SNEC/SNUC (P value = 0.00071), and NKSCC/SNUC (P value = 3.2E−08). (d) A ROC curve and AUC of the model containing the first and second components; AUC was calculated for comparison of one class to the others, resulting in NKSCC vs (SNEC and SNUC) AUC = 0.954, SNEC vs (SNUC and NKSCC) AUC = 1, and SNUC vs (NKSCC and SNEC) AUC = 0.973.

genes: *DSG2* and *TMEM123* (sPLS-DA, first component, see Table 2) for NKSCC, *NRSN1*, and *TAGLN3* (sPLS-DA, first component, see Table 2), for SNEC and *RGS1* (sPLS-DA, second component, see Table 2) and *CD8A* ($CD8^+$ effector memory T cells according to microenvironment analysis) for SNUC, and *ACTB* as housekeeping genes. As presented in Fig. A3, the selective expression revealed by gene expression analysis was confirmed by RT-qPCR (up-regulation in NKSCC: DSG2 and TMEM123 P value = 0.023 and P value = 0.019, respectively; up-regulation in SNEC: NRSN1 and TAGLN3 P value = 0.0054 and P value = 0.032, respectively; up-regulation in SNUC: RGS1 and CD8A, P value = 0.0094 and P value = 0.016, respectively; p-values by Kruskal–Wallis test).

Functional annotation

The biological pathways related to the histological subtype were investigated by GSEA. The latter revealed the regulatory relations among genes and provided a systematic understanding of the underlying molecular mechanisms. According to the separation obtained by sPLS-DA, we decided to compare SNEC, SNUC, and NKSCC each to the combined remaining two histological subtypes. GSEA revealed that only one gene set was upregulated in “SNEC vs other subtypes,” in contrast to the large number of gene sets (N = 20) upregulated in “SNUC vs other subtypes” and the mild upregulation of gene sets (N = 6) in NKSCC (Table A3; most relevant ones are highlighted in Table 2).

Neuroendocrine content

We focused our attention on estimating the proportion of neuroendocrine cells in each sample by means of CIBERSORT, a computational tool able to infer the proportion of a cellular type from bulk gene expression data. Our sPLS-DA identified a list of 72 genes that stratify SNEC from the other subtypes. This gene list, named “First Component List” (Fig. 4a) served as a gene signature for assessing the neuroendocrine involvement (Fig. 4b) in each sample of our case

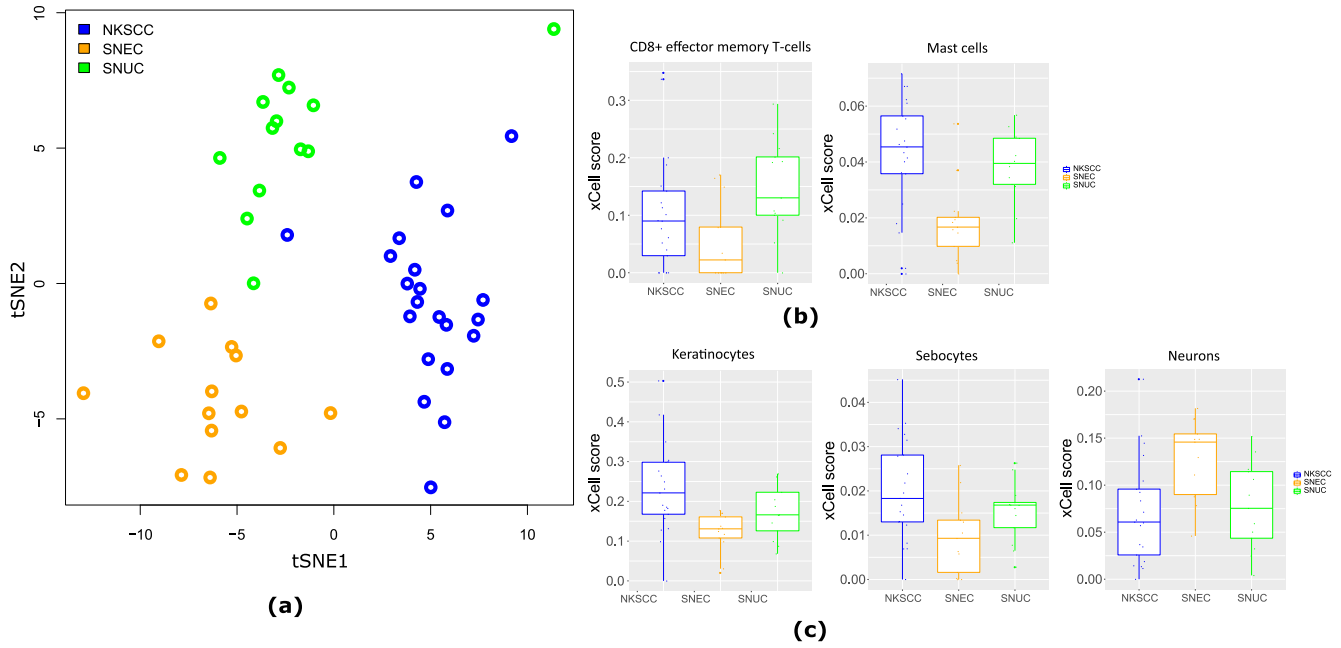

Fig. 3. The tumor microenvironment. (a) Visualization of infiltrates of the immune and "other cells" in SNCs as assessed by xCell; individual patients are summarized based on two-dimensional coordinates from t-distributed stochastic neighbor embedding (t-SNE) and are colored by subtype. (b) Immune-cell infiltrates; the box plot shows the transformed xCell scores for $CD8^+$ effector memory T cells and mast cells showing a different proportion among the histological subtypes, yielding P value = 0.014 and P value = 0.00241, respectively. (c) Other cell infiltrates; the box plot shows the transformed xCell scores for neurons, keratinocytes, and sebocytes (P value = 0.00612, P value = 0.00249, and P value = 0.0135, respectively). P values were calculated by the Kruskal–Wallis test. It is noteworthy that the scores of mast cells and sebocytes, which reflect the true cell proportions in the tumor microenvironment, are lower compared to the others, and they should be interpreted with caution.

material. The neuroendocrine involvement reflected the relative abundance (proportion) of neuroendocrine cells in the tumor tissues as a score ranging from 0 (i.e., absence) to 1 (i.e., exclusive presence). As expected, SNEC tumors showed the strongest neuroendocrine involvement, median = 0.957 (range: 0.502–1.000) as compared to the other histological subtypes, whereas NKSCC and SNUC showed weak neuroendocrine involvement (NKSCC median = 0.14, range: 0–0.657; SNUC median = 0.0555, range: 0–0.539) with the exception of two cases with the neuroendocrine-cell proportion > 0.5. Besides our analysis, we tested an additional novel signature generated by Chen et al. This recent Pan-cancer analysis, including head and neck cancers [22], provided a neuroendocrine signature, named the C4 subtype, for the identification of the neuroendocrine subclass of tumors. Therefore, the Pan-cancer neuroendocrine signature was tested in our dataset for comparison purposes. The signature was composed of 169 genes. Genes were annotated by gene symbol and Entrez Gene ID, and 134 out of 169 of genes typical for the C4 subtype were present in our gene expression data matrix (see Table A2). Pan-cancer C4 subtype gene expression was summarized by z-score to obtain a composite index, and the resulting heatmap is depicted in Fig. A4. Our neuroendocrine involvement score and Pan-cancer C4 subtype signature revealed a significant positive correlation (r = 0.727, P value = 3.71E−09). However, the performance of the Pan-cancer C4 subtype signature on separating SNEC was worse if compared to our First Component List signature: the Pan-cancer signature identified 11 of 13 SNECs as neuroendocrine, in contrast to our First Component List signature, which classified 13 of 13 SNECs as neuroendocrine tumors (as summarized in Table 2).

Discussion

Histological diagnosis of SNCs is often complex due to the presence of overlapping characteristics and similar patterns. High-throughput technologies have proved to have a great potential for providing insights into tumor biology. We chose to reduce the analysis to three histological subtypes of epithelial origin sharing some morphological characteristics (NKSCC, SNEC, and SNUC) to which we applied in-depth molecular analyses. This analysis could have practical applications in those cases where it is difficult to differentiate among these histotypes because they may have overlapping morphological features; in this regard, the sinonasal tract has the highest rate of discrepant diagnoses among the head and neck subsites [6].

The initial sPLS-DA analysis provided evidence that the three SNC subtypes were clearly separated, and the subsequent xCell tumor microenvironment, functional pathway, and neuroendocrine content analyses confirmed that this separation, thereafter discussed for each subtype, was a reflection of their intrinsic molecular patterns. In the case of NKSCC, different genes were significantly expressed in the sPLS-DA "First Component," in particular desmoglein 2 (*DSG2*, a desmosomal cadherin) and the keratinocyte-associated transmembrane protein 3 (*TMEM123*). These expressed genes indicated that NKSCC, despite the minimal or absent squamous differentiation, maintained markers of keratinization, and *DSG2* has often been found to be overexpressed in HNSCCs [23]. In agreement with this observation, according to microenvironment analysis, the proportion of "keratinocytes" in NKSCC, in this case representative of epithelial tumor cells, was significantly higher than that in the other two subtypes, while neuroendocrine involvement was low. In this subtype, the same analysis revealed a relative increase in the proportions of mast cells and sebocytes; however, this observation—because of the very small detectable input—should be interpreted with caution and needs external validation. For NKSCC, functional analyses highlighted a significant upregulation of pathways associated with altered signaling and proliferation (MYC targets, mitotic spindle, and WNT–β-catenin signaling). Among these, MYC targets may be potentially druggable; in fact, even if direct targeting of this gene has not yet been identified, several indirect ways of pharmacological targeting of MYC are possible [24]. In the case of SNEC, as expected, sPLS-DA indicated that this subtype overexpressed i) brain or adrenal markers including *NRSN1* and *TAGLN3*

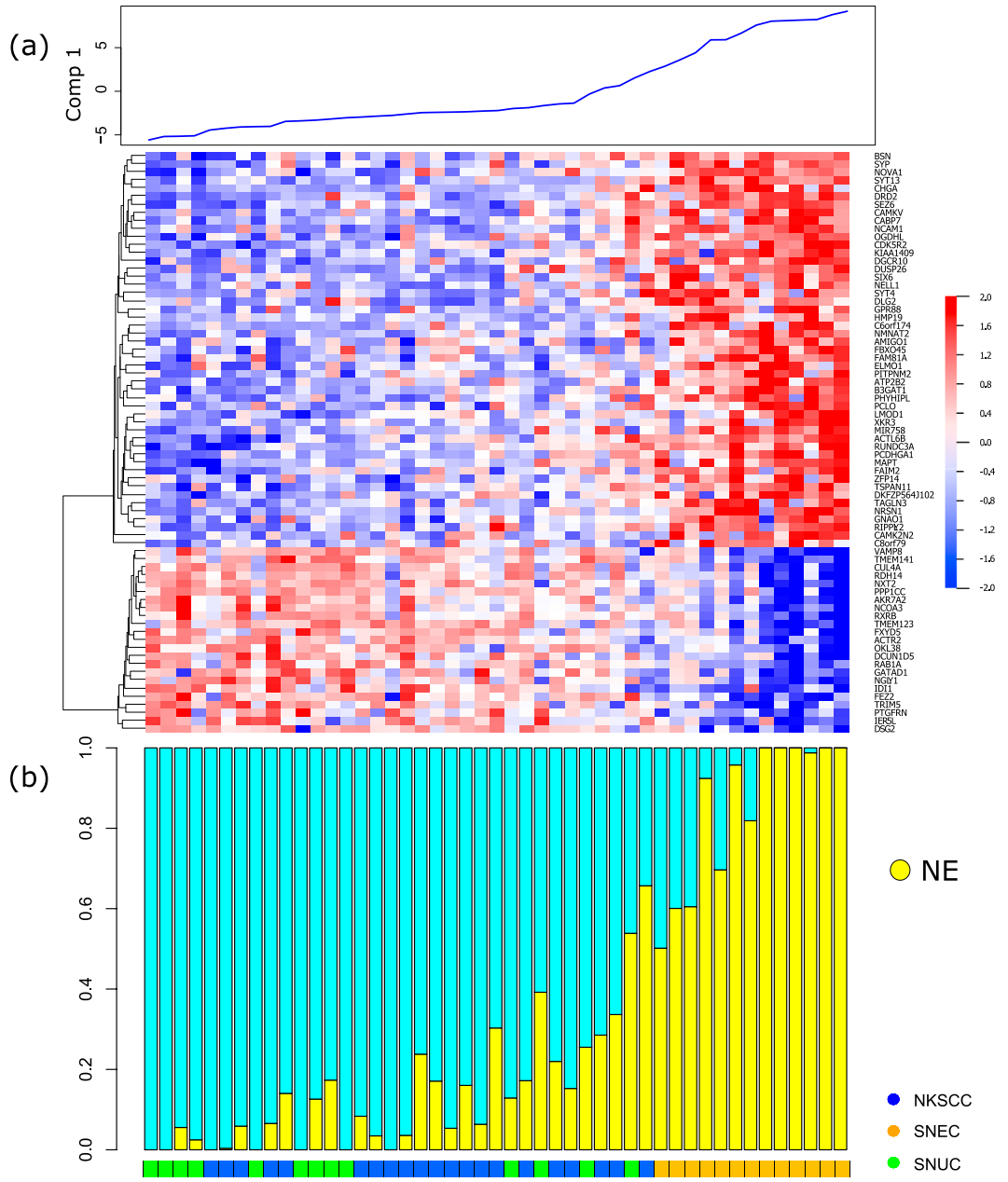

Fig. 4. Neuroendocrine involvement. (a) A heatmap of the 72 genes of sPLS-DA discriminating SNEC from the other histological subtypes; the samples are ordered by first component values as shown in the line chart. Forty-nine genes show an upregulation trend in SNEC tumors, whereas 23 upregulation in histological subtypes other than SNEC, corresponding to the genes having positive or negative loading values in Table A1, respectively. (b) Neuroendocrine involvement was assessed by CIBERSORT using the 72-gene sPLS-DA first component as an input custom signature and providing the proportion of neuroendocrine cells (yellow bars). Fifteen samples, including all the SNEC tumors, one NKSCC, and one SNUC, yielded a score > 0.5.

found in brain tissue (https://www.uniprot.org); ii) neuroendocrine markers including *SYT13*, which is reported to be overexpressed in other neuroendocrine tumors, such as those of bowel and stomach, and is known to be associated with peritoneal metastases and to be a potential target for treatment [25,26], and *SYP* and *CHGA*, used for IHC diagnosis of neuroendocrine differentiation in breast and digestive system cancers [27,28]. In addition, microenvironment analysis detected a high proportion of the "neuronal component," which confirmed the upregulation of brain markers. For this subtype, the functional analysis was not helpful; in fact, a single pathway associated with pancreatic β-cells was upregulated, reinforcing once again the relevant endocrine involvement.

As for SNUC, the sPLS-DA second component highlighted the overexpression of *RGS1*, a member of the regulators of the G protein signaling family, involved in multiple immune-system–mediated diseases and upregulated in HNSCC metastases [29,30]. It has been observed that RGS1 regulates chemokine signaling [31], thereby connecting *RGS1* upregulation to our results on deregulation in functional immune pathways seen in SNUC samples. Recently, *RGS1* expression was proposed as a prognostic marker for risk stratification and as a promising target for the development of therapeutic strategies against multiple myeloma [31]. The microenvironment analysis uncovered low-to-moderate epithelial or endocrine differentiation but a well-defined immune profile. In particular, SNUC tumors turned out to contain a high proportion of $CD8^+$ effector memory cells according to the microenvironment analysis and a strong association with immune-

system–related functional pathways. These pathways shared several upregulated subgroups of chemokines including CXCL10, CXCL11, and CCL19. Other upregulated functional pathways, such as epithelial–mesenchymal transition, the TP53 pathway, the KRAS pathway, and hypoxia, were found to be enhanced similarly to HNSCC with a poor prognosis [32]. Furthermore, upregulation of genes involved in the hallmarks of cholesterol homeostasis was observed; this observation deserves further in-depth evaluation, in light of the *miR758* deregulation in SNEC, demonstrated to be involved in the same pathway [33]. Overall, the observed gene expression profile makes SNUC a possible candidate for immunotherapeutic strategies, being more prone to elicit an immune response. A better characterization of the profile of the $CD8^+$ T cells [34] could help to identify the most effective treatment approach to SNUC, fully taking advantage of the possible synergism of chemotherapy and immunotherapy [35].

Of note, the neuroendocrine involvement of our entire case material was analyzed via two different signatures: the first signature (generated in the present study) and the second signature, named the Pan-cancer C4 subtype [20] (generated on over 10,000 samples from 32 cancer types and associated with central nervous system and neuroendocrine involvement). A very small overlap of the two gene lists was noted: only five genes (*CHGA*, *PHYHIPL*, *SYT13*, *SYT4*, and *TAGLN3*) were in common, and at least three of them are among the most frequently used in IHC for differential diagnosis. Our first component signature well separated SNEC from the other two SNC subtypes: all SNEC samples manifested more than 50% of neuroendocrine involvement, whereas 20% of NKSCCs and 23% of SNUC samples demonstrated a proportion of neuroendocrine involvement up to 25%. In contrast, the Pan-cancer C4 signature yielded a heterogeneous pattern in which NKSCC and SNUC were widely distributed, and SNEC, although more strongly associated with high expression of the neuroendocrine signature, was not sufficiently discriminated. Possible explanations of the different performance of the two signatures are as follows: the high performance of the sPLS-DA first component may be caused by the overfitting due to the use of the same case material for generating and testing; the C4 performance may be explained by the large heterogeneity of the Pan-cancer tumor samples. From a clinical point of view, the finding that neuroendocrine traits are present also in a percentage of NKSCC and SNUC cases should prompt a better investigation of these cases. Further studies should be conducted to assess whether these traits retain a prognostic value or could also be a druggable target.

We should acknowledge the limitations of this study. First, with the samples derived from diagnostic biopsies, there is a risk of having dissected a portion of the disease, without considering the heterogeneity of the tumor. The analysis of multiple regions from the whole resected tumor remains the optimal way to assess tumor heterogeneity; however, in an attempt to determine the histological subtype and possibly the best combination of treatment modalities for SNCs, we should often rely on diagnostic biopsies. Second, we focused only on the transcriptome analysis on a platform well suited for FFPE samples [14] but limited to the expression of coding RNA, while other classes of RNA, and in particular long noncoding RNAs (lncRNAs), microRNAs (miRNAs), and circular RNAs (circRNAs), emerged as critical regulators of cancer-related pathological changes not only in post-transcriptional regulation of oncogenes and tumor suppressors but also in interactions or competitive interaction with each other [36,37]. As proof of their potential role in SNC biology, we identified deregulation of noncoding RNA, such as miR758, in SNEC and LINC00461 (econexin) in SNUC, the latter being recently described as a potential oncogene in glioma [38]. Therefore, we plan not only to analyze new independent case materials but also to adopt more recently established platforms for gene expression enabling simultaneous evaluation of coding and noncoding RNA.

In conclusion, the gene expression analysis of three SNC entities (NKSCC, SNEC, and SNUC) revealed a good diagnostic ability to differentiate these histotypes. In parallel, it revealed some characteristics that are partially shared by the different histotypes. For instance, the neuroendocrine pathway, typical and pathognomonic of SNEC, is also present at lower levels of expression in NKSCC and SNUC and could be useful if analyzed during the pathological diagnosis of SNCs. Moreover, the genomic pathways we discovered could help to find prognostic and therapeutic opportunities to increase the chances of a cure of SNCs. In this regard, identification of immune pathways in SNUC and NKSCC should be further investigated, for possible integration of immunotherapy into the multidisciplinary approach to these cancers. In general, molecular profiling of SNCs could pave the way for a more personalized treatment of these diseases, considering the global dismal prognosis and the lack of new drugs studied for this rare cancer. All these biological interpretations based on gene expression analysis and internal RT-qPCR require further independent validation studies, and these are being performed on an independent cohort whose compilation is in progress (SINTART trials; Clinicaltrials.gov identifier: NCT02099175 and NCT02099188).

Author contributions

Conceptualization, P.B., L.L., and L.D.-C.; methodology, P.B. and L.D.-C.; case material selection, recruitment, and formal analysis, C.F., R.G., E.O., C.F., L.L., C.P., E.M., F.P., S.P., P.Q., F.S., M.T.-Z., P.B., P.C., P.A., and P.B.; ethical aspects: P.B., L.L.; data curation, P.B., M.-S.S., S.C., and L.D.-C.; writing (original draft preparation), P.B., M.-S.S., S.C., and L.D.-C.; writing (review & editing), L.D.-C., M.-S.S., C.F., R.G., E.O., C.F., L.L., C.P., E.M., F.P., S.P., P.Q., F.S., M.T.-Z., P.B., P.C., P.A., S.C., and P.B.; and funding acquisition, P.B.

Funding

This study was partially supported by Associazione Italiana Ricerca Cancro (AIRC) grant number IG 17422 to P.B.

Acknowledgments

The authors wish to thank the Platform of Integrated Biology of Fondazione IRCCS Istituto Nazionale dei Tumori for support in the genomic analysis.

Conflicts of interest

The authors declare no conflicts of interest. The funders had no role in the design of the study; in the collection, analyses, or interpretation of data; in the writing of the manuscript, and in the decision to publish the results.

Appendix A. Supplementary material

Supplementary data to this article can be found online at https://doi.org/10.1016/j.oraloncology.2019.02.003.

References

[1] El-Naggar AK, Chan JKC, Grandis JR, Takata T, Slootweg PJ. WHO classification of head and neck tumours, 4th ed., vol. 9. Lyon, France: IARC; 2017.
[2] López-Hernández A, Vivanco B, Franchi A, Bloemena E, Cabal VN, Potes S, et al. Genetic profiling of poorly differentiated sinonasal tumour. Sci Rep 2018;8(1):3998. https://doi.org/10.1038/s41598-018-21690-6.
[3] RARECARE – Surveillance of Rare Cancers in Europe. Available online: www.rarecare.eu.
[4] Tuner JH, Reh DD. Incidence and survival in patients with sinonasal cancer: a historical analysis of population-based data. Head Neck 2012;34:877–85. https://doi.org/10.1002/hed.21830.
[5] Llorente JL, Lopez F, Suáre C, Hermsen MA. Sinonasal carcinoma: clinical, pathological and genetic advances for new therapeutic opportunities. Nat Rev Clin Oncol 2014;11:460–72. https://doi.org/10.1038/nrclinonc.2014.97.
[6] Mehrad M, Chernock RD, El-Mofty SK, Lewis Jr. JS. Diagnostic discrepancies in mandatory slide review of extradepartmental head and neck cases: experience at a large academic center. Arch Pathol Lab Med 2015;139(12):1539–45. https://doi.

org/10.5858/arpa.2014-0628-OA.
[7] Stathis A, Zucca E, Bekradda M, Gomez-Roca C, Delord JP, de La Motte Rouge T, et al. Clinical response of carcinomas harboring the BRD4-NUT oncoprotein to the targeted bromodomain inhibitor OTX015/MK-8628. CancerDiscov 2016;6(5):492–500. https://doi.org/10.1158/2159-8290.CD-15-1335.
[8] Udager AM, Rolland DCM, McHugh JB, Betz BL, Murga-Zamalloa C, Carey TE, et al. High-frequency targetable EGFR mutations in sinonasal squamous cell carcinomas arising from inverted sinonasal papilloma. Cancer Res 2015;75(13):2600–6. https://doi.org/10.1158/0008-5472.CAN-15-0340.
[9] Frierson Jr HF, Mills SE, Fechner RE, Taxy JB, Levine PA. Sinonasal undifferentiated carcinoma. An aggressive neoplasm derived from schneiderian epithelium and distinct from olfactory neuroblastoma. Am J Surg Pathol 1986 Nov;10(11):771–9.
[10] El-Naggar AK, Chan JKC, Grandis JR, Takata T, Slootweg PJ. WHO classification of tumours, 4th ed., vol. 9. Lyon: Edited lnternational Agency for Research on Cancer; 2017.
[11] Edge SB, Compton CC. The American Joint Committee on Cancer: the 7th edition of the AJCC cancer staging manual and the future of TNM. Ann Surg Oncol 2010;17:1471–4. https://doi.org/10.1245/s10434-010-0985-4.
[12] Mittempergher L, de Ronde JJ, Nieuwland M, Kerkhoven RM, Simon I, Rutgers EJ, et al. Gene expression profiles from formalin fixed paraffin embedded breast cancer tissue are largely comparable to fresh frozen matched tissue. PLoS One 2011;6(2):e17163. https://doi.org/10.1371/journal.pone.0017163.
[13] Ravo M, Mutarelli M, Ferraro L, Grober OM, Paris O, Tarallo R, et al. Quantitative expression profiling of highly degraded RNA from formalin-fixed, paraffin-embedded breast tumor biopsies by oligonucleotide microarrays. Lab Invest 2008;88(4):430–40. https://doi.org/10.1038/labinvest.2008.
[14] Bossi P, Bergamini C, Siano M, Cossu Rocca M, Sponghini AP, Favales F, et al. Functional genomics uncover the biology behind the responsiveness of head and neck squamous cell cancer patients to Cetuximab. Clin Cancer Res 2016;22:3961–70. https://doi.org/10.1158/1078-0432.CCR-15-2547.
[15] National Center for Biotechnology Information. Available online: www.ncbi.nmlm.nih.gov/projects/geo/.
[16] Bioconductor. Available online: www.bioconductor.org.
[17] Chambers KJ, Lehmann AE, Remenschneider A, Dedmon M, Meier J, Gray ST, et al. Incidence and survival patterns of sinonasal undifferentiated carcinoma in the United States. J Neurol Surg B Skull Base 2015;76(2):94–100. https://doi.org/10.1055/s-0034-1390016.
[18] Patel TD, Vazquez A, Dubal PM, Baredes S, Liu JK, Eloy JA. Sinonasal neuroendocrine carcinoma: a population-based analysis of incidence and survival. Int Forum Allergy Rhinol 2015;5(5):448–53. https://doi.org/10.1002/alr.21497.
[19] Unsal AA, Dubal PM, Patel TD, Vazquez A, Baredes S, Liu JK, et al. Squamous cell carcinoma of the nasal cavity: a population-based analysis. Laryngoscope 2016;126(3):560–5. https://doi.org/10.1002/lary.25531.
[20] Bersanelli M, Mosca E, Remondini D, Giampieri E, Sala C, Castellani G, et al. Methods for the integration of multi-omics data: mathematical aspects. BMC Bioinform 2016;17(Suppl 2):15. https://doi.org/10.1186/s12859-015-0857-9.
[21] De Cecco L, Giannoccaro M, Marchesi E, Bossi P, Favales F, Locati LD, et al. Integrative miRNA-gene expression analysis enables refinement of associated biology and prediction of response to Cetuximab in head and neck squamous cell cancer. Genes (Basel) 2017;8(1):E35. https://doi.org/10.3390/genes8010035.
[22] Chen F, Zhang Y, Gibbons DL, Deneen B, Kwiatkowski DJ, Ittmann M, et al. Pan-cancer molecular classes transcending tumor lineage across 32 cancer types, multiple data platforms, and over 10,000 cases. Clin Cancer Res 2018;24(9):2182–93. https://doi.org/10.1158/1078-0432.CCR-17-3378.
[23] Overmiller AM, Pierluissi JA, Wermuth PJ, Sauma S, Martinez-Outschoorn U, Tuluc M, et al. Desmoglein 2 modulates extracellular vesicle release from squamous cell carcinoma keratinocytes. FASEB J 2017;31(8):3412–24. https://doi.org/10.1096/fj.201601138RR.
[24] Chen H, Liu H, Qing G. Targeting oncogenic Myc as a strategy for cancer treatment. Signal Transduct Target Ther 2018;3:5. https://doi.org/10.1038/s41392-018-0008-7.
[25] Keck KJ, Breheny P, Braun TA, Darbro B, Li G, Dillon JS, et al. Changes in gene expression in small bowel neuroendocrine tumors associated with progression to metastases. Surgery 2018;163(1):232–9. https://doi.org/10.1016/j.surg.2017.07.031.
[26] Kanda M, Shimizu D, Tanaka H, Tanaka C, Kobayashi D, Hayashi M, et al. Synaptotagmin XIII expression and peritoneal metastasis in gastric cancer. Br J Surg 2018;105(10):1349–58. https://doi.org/10.1002/bjs.10876.
[27] Rosen LE, Gattuso P. Neuroendocrine tumors of the breast. Arch Pathol Lab Med 2017;141(11):1577–81. https://doi.org/10.5858/arpa.2016-0364-RS.
[28] Inzani F, Petrone G, Fadda G, Rindi G. Cyto-histology in NET: what is necessary today and what is the future? Rev Endocr Metab Disord 2017;18(4):381–91. https://doi.org/10.1007/s11154-017-9428-x.
[29] Xie Z, Chan EC, Druey KM. R4 regulator of G protein signaling (RGS) proteins in inflammation and immunity. AAPS J 2016;18(2):294–304. https://doi.org/10.1208/s12248-015-9847-0.
[30] Liu CJ, Liu TY, Kuo LT, Cheng HW, Chu TH, Chang KW, et al. Differential gene expression signature between primary and metastatic head and neck squamous cell carcinoma. J Pathol 2008;214(4):489–97. https://doi.org/10.1002/path.2306.
[31] Roh J, Shin SJ, Lee AN, Yoon DH, Suh C, Park CJ, et al. RGS1 expression is associated with poor prognosis in multiple myeloma. J Clin Pathol 2017;70(3):202–7. https://doi.org/10.1136/jclinpath-2016-203713.
[32] De Cecco L, Nicolau M, Giannoccaro M, Daidone MG, Bossi P, Locati L, et al. Head and neck cancer subtypes with biological and clinical relevance: meta-analysis of gene-expression data. Oncotarget 2015;6(11):9627–42.
[33] Li BR, Xia LQ, Liu J, Liao LL, Zhang Y, Deng M, et al. miR-758-5p regulates cholesterol uptake via targeting the CD36 3'UTR. Biochem Biophys Res Commun 2017;494(1–2):384–9. https://doi.org/10.1016/j.bbrc.2017.09.150.
[34] Weng NP, Araki Y, Subedi K. The molecular basis of the memory T cell response: differential gene expression and its epigenetic regulation. Nat RevImmunol 2012;12(4):306–15. https://doi.org/10.1038/nri3173.
[35] Yan Y, Cao S, Liu X, Harrington SM, Bindeman WE, Adjei AA, et al. CX3CR1 identifies PD-1 therapy-responsive CD8+ T cells that withstand chemotherapy during cancer chemoimmunotherapy. JCI Insight 2018;3(8):97828. https://doi.org/10.1172/jci.insight.97828.
[36] Anastasiadou E, Faggioni A, Trivedi P, Slack FJ. The nefarious nexus of noncoding RNAs in cancer. Int J Mol Sci. 2018;19(7):E2072. https://doi.org/10.3390/ijms19072072.
[37] Anastasiadou E, Jacob LS, Slack FJ. Non-coding RNA networks in cancer. Nat Rev Cancer 2018;18:5–18. https://doi.org/10.1038/nrc.2017.99.
[38] Deguchi S, Katsushima K, Hatanaka A, Shinjo K, Ohka F, Wakabayashi T, et al. Oncogenic effects of evolutionarily conserved noncoding RNAECONEXIN on gliomagenesis. Oncogene 2017;36(32):4629–40. https://doi.org/10.1038/onc.2017.88.